

R. Scaramella

INAF Osservatorio di Roma

-SKAItaly June 2012-

Old timer...

Interested since long in two fascinating projects:

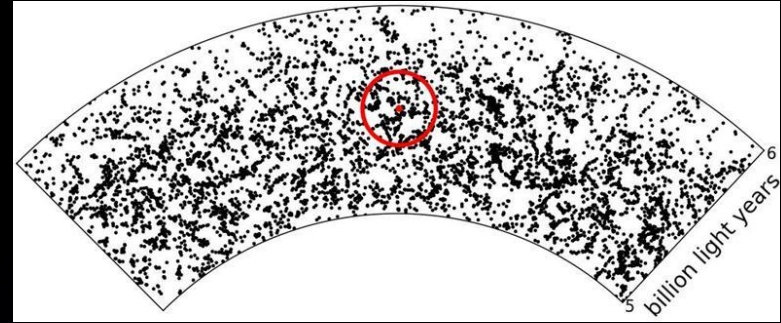
- Italian involvement in **SKA** (SKADS, prepSKA, SKA day 2006, etc)

- Italian involvement in **Euclid**

(since the beginning on the imaging side, currently Mission Survey Scientist;
Euclid material from/thanks the Euclid Consortium)

Giga structures...

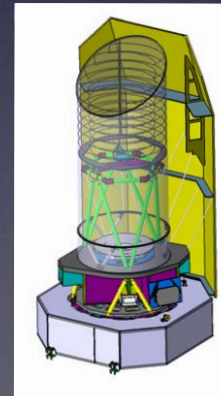
Giga samples, *giga*€



- observed with:

- ✦ a **Mega** telescope: $\sim 1,000,000 \text{ m}^2$

- ✦ a **mini** telescope: $\sim 1 \text{ m}^2$

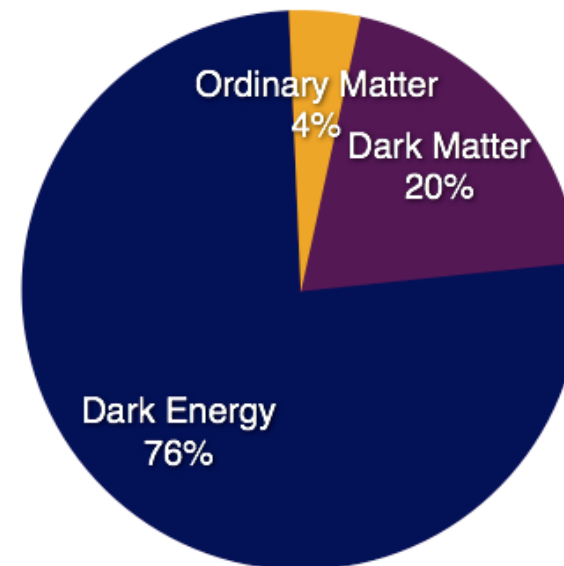
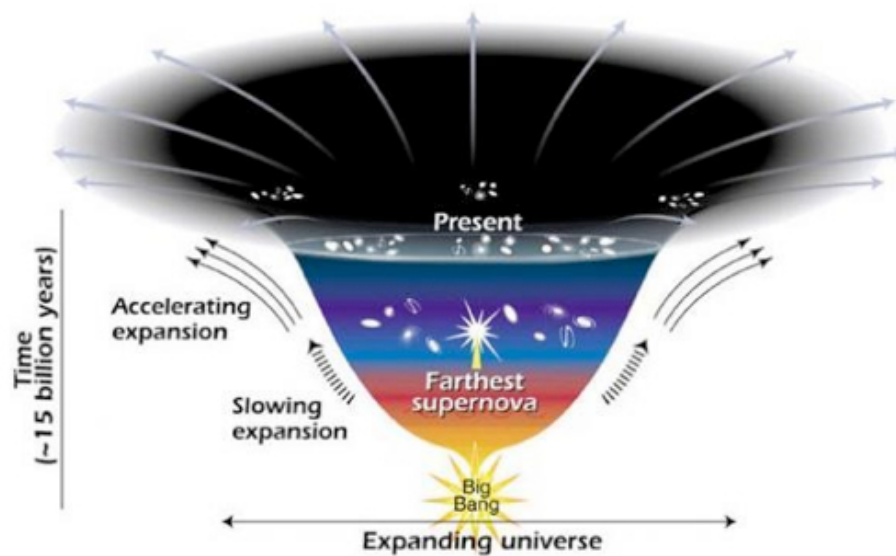


Open Questions in Cosmology

- **Nature of the Dark Energy**
- Nature of the Dark Matter
- Initial conditions (Inflation Physics)
- **Modifications to Gravity**
- Formation and Evolution of Galaxies

**Large ignorance on
> 95% of Universe
content !?**

“precise” ignorance



New Worlds, New Horizons in Astronomy and Astrophysics (Decadal Survey 2010)

Ground Projects – Large – in Rank Order

Large Synoptic Survey Telescope (LSST)

LSST is a multipurpose observatory that will explore the nature of dark energy and the behavior of dark matter, and will robustly explore aspects of the time-variable universe that will certainly lead to new discoveries. LSST addresses a large number of the science questions highlighted in this report. An 8.4-meter optical telescope to be sited in Chile, LSST will image the entire available sky every 3 nights.

TABLE ES.3 Ground: Recommended Activities—Large Scale (Priority Order)

Recommendation ^b	Science	Technical Risk ^c	Appraisal of Costs Through Construction ^a (U.S. Federal Share 2012-2021)	Appraisal of Annual Operations Costs ^d (U.S. Federal Share)	Page Reference
1. LSST - Science late 2010s - NSF/DOE	Dark energy, dark matter, time-variable phenomena, supernovas, Kuiper belt and near Earth objects	Medium low	\$465M (\$421M)	\$42M (\$28M)	7-29

Space Projects – Large – in Rank Order

Wide Field Infrared Survey Telescope (WFIRST)

A 1.5-meter wide-field-of-view near-infrared-imaging and low-resolution-spectroscopy telescope, WFIRST will settle fundamental questions about the nature of dark energy, the discovery of which was one of the greatest achievements of U.S. telescopes in recent years. It will employ three distinct techniques—measurements of weak gravitational lensing, supernova distances, and baryon acoustic oscillations—to determine the effect of dark energy on the evolution of the universe. An equally

TABLE ES.5 Space: Recommended Activities—Large-Scale (Priority Order)

Recommendation	Launch Date ^b	Science	Technical Risk ^c	Appraisal of Costs ^a		Page Reference
				Total (U.S. share)	U.S. share 2012-2021	
1. WFIRST - NASA/DOE collaboration	2020	Dark energy, exoplanets, and infrared survey-science	Medium low	\$1.6B	\$1.6B	7-17

DE as TOP priority both for Ground and Space also across the Atlantic

Current status of Dark Energy

Dark Energy:

- Affects cosmic geometry and structure growth
- Parameterized by equation of state parameter:

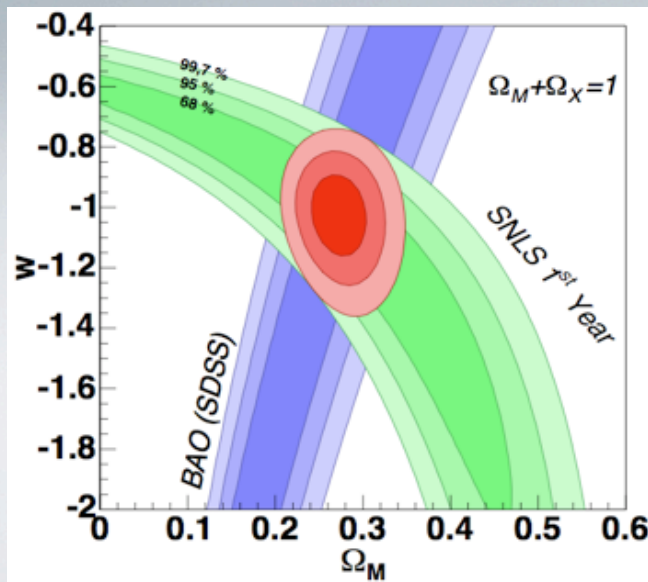
$w(z)=p/\rho$, constant $w=-1$ for cosmological constant

Not necessarily DE!!!
could be non std GR

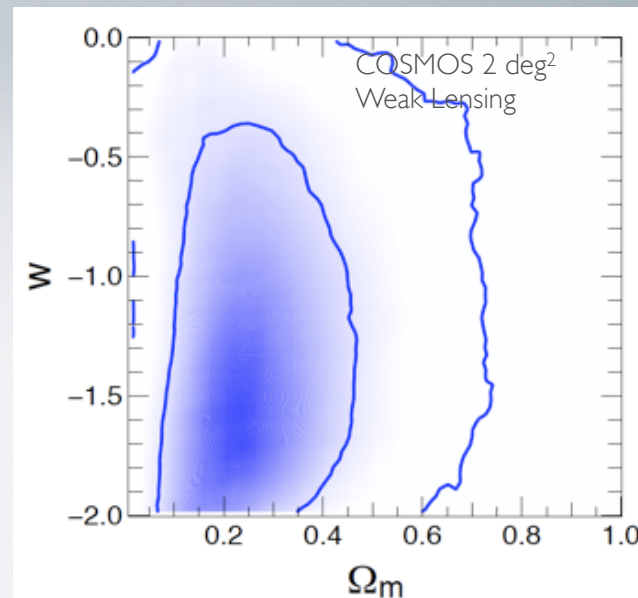
Current constraints: 10% error on constant w

For “definite” answers on DE: need to reach a precision of 1% on (varying) w and 10% on $w_a=dw/da$ → Objective for Euclid alone (FoM ~ 4-500)

Astier et al. 2005



Schrabback et al 2009



Recall a few basics

$$H^2(a) \equiv \left(\frac{\dot{a}}{a}\right)^2 = H_0^2 \left[\Omega_m a^{-3} + \Omega_r a^{-4} + \Omega_k a^{-2} + \Omega_x a^{-3(1+w)} \right]$$

Evolution governed by components: $H(z) \Leftrightarrow \Omega_x, w$

$$H^2(a) = H_0^2 \left[\Omega_R a^{-4} + \Omega_M a^{-3} + \Omega_k a^{-2} + \Omega_{DE} \exp \left\{ 3 \int_a^1 \frac{da'}{a'} [1 + w(a')] \right\} \right]$$

Ellipses: uncertainty in parameters via Fisher matrix. An useful approximation

(curse of dimensionality; also different definitions & priors).

Usually use Figure of Merit = 1/Area

$$FoM = 1/(\Delta w_0 \times \Delta w_a)$$

$a=(1+z)^{-1}$ expansion factor

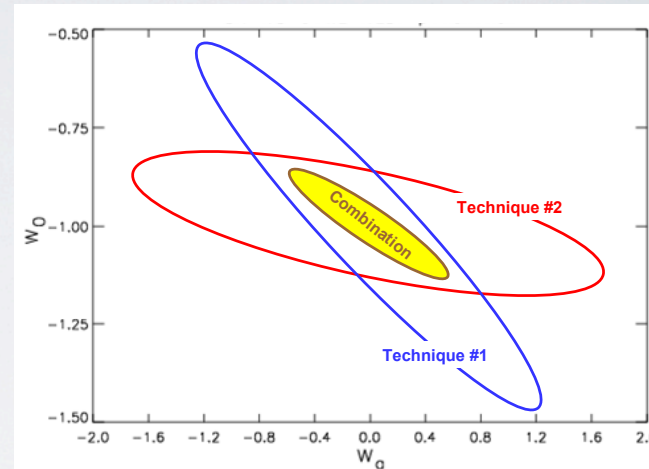
δ = density fluctuation

$P(k)$ = power spectrum of $\delta(\mathbf{x}, z)$

$w = p/\rho, \gamma = \text{growth index}$

$$w(z) = w_0 + w_a (1-a) \quad f_{GR}(z) \equiv \frac{d \ln G_{GR}}{d \ln a} \approx [\Omega_m(z)]^\gamma$$

Λ : $w_0 = -1, w_a = 0; \gamma \sim 0.55$



to get a small uncertainty on power spectrum need:

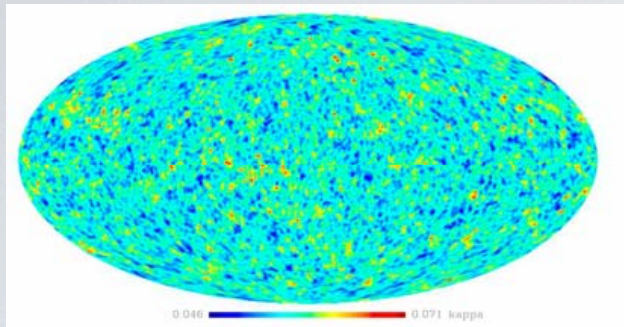
$$\frac{\sigma}{P} = \sqrt{\frac{2}{n_{\text{modes}}}} \left(1 + \frac{1}{P \bar{n}} \right)$$

accurate/adequate sampling in number of objects

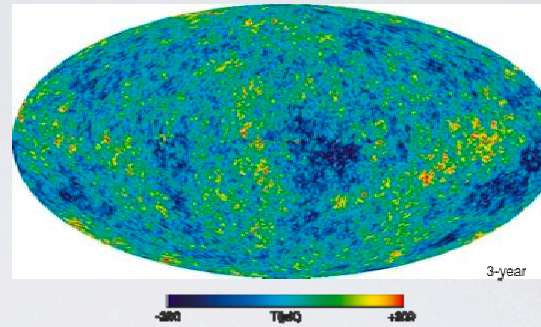
large volumes to accommodate several Fourier modes

Cosmic Variance \Leftrightarrow Volume
Poisson \Leftrightarrow Number

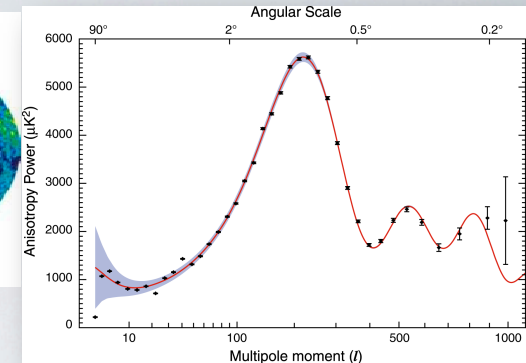
Synergy with Planck: Universe @ $z \sim 1000$ vs $z \sim 1-3$



Weak Lensing Dark Matter Maps



CMB Temperature Maps (5y WMAP)



Oscillations

Figure 2.15: a. (left) Simulated all sky mass map from weak lensing (Teyssier et al., 2008) for a Euclid survey. This was produced using a 70 billion particle N-Body simulation. This can be compared with the all sky temperature maps of the CMB, such as the WMAP 5 Year all sky temperature map (Hinshaw et al., 2008). b. (right) The Planck CMB map will produce an all sky temperature map at an even higher resolution of approximately 0.2 degrees at a redshift of ~ 1100 . Euclid will produce a 3D map between a redshift of 0 and 2 down to **arcminute scales**.

-if- most of the effects happens at $z < 3$

Need also dynamics to further disentangle

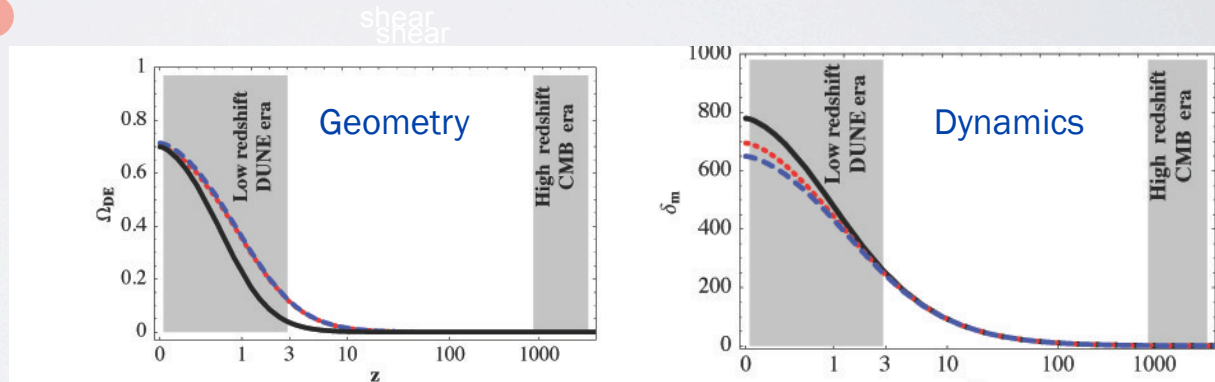


Figure C.1: Effect of dark energy on the evolution of the Universe. **Left:** Fraction of the density of the Universe in the form of dark energy as a function of redshift z , for a model with a **cosmological constant ($w=-1$, black solid line)**, dark energy with a different equation of state ($w=-0.7$, red dotted line), and a modified gravity model (blue dashed line). In all cases, dark energy becomes dominant in the low redshift Universe era probed by DUNE, while the early Universe is probed by the CMB. **Right:** Growth factor of cosmic structures for the same three models. **Only by measuring the geometry (left panel) and the growth of structure (right panel) at low redshifts can a modification of dark energy be distinguished from that of gravity. Weak lensing measures both effects.**

Does gravity follow standard G.R.?

Weak
limit

Need experiments with high sensitivity/precision....

$$w \equiv p/\rho \quad w(a) = w_p + (a_p - a)w_a \quad \frac{d \log \delta_m}{d \log a} \equiv f(a) \cong \Omega_m(a)^\gamma$$

$$ds^2 = a(\tau)^2 [-(1 + 2\psi)d\tau^2 + (1 - 2\phi)dr^2]$$

e.g. $f(R)$ in
Lagrangian

$$R = g^{\mu\nu} R_{\mu\nu}$$

$$S[g] = \int \frac{1}{2\kappa} R \sqrt{-g} d^4x$$

$$S[g] = \int \frac{1}{2\kappa} f(R) \sqrt{-g} d^4x$$

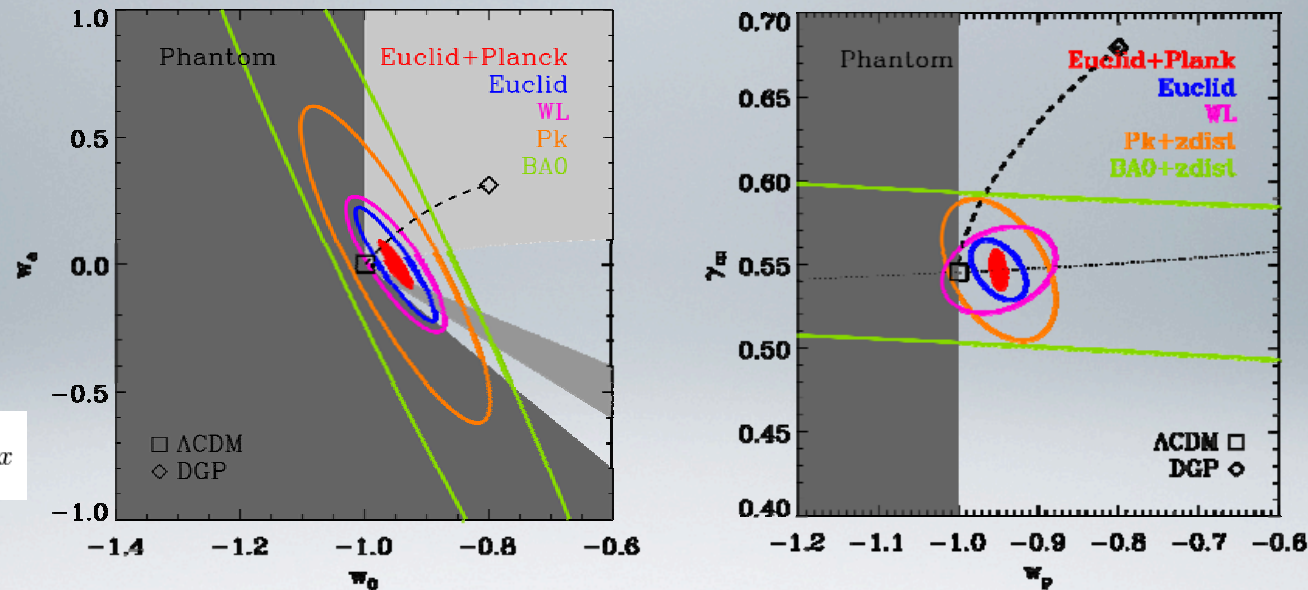


Figure 2.13: a. (left) Predicted constraints from Euclid on the dark energy w_0 - w_a plane. The grey areas show different region relevant for DE theory. The darkest grey region $w_0 < -1$ is the Phantom zone, while the others show 'thaw' and 'freeze' models (middle grey and lightest grey). The outer (green) ellipses show the constraints from BAO, orange shows the galaxy power spectrum, $P(k)$, purple weak lensing alone, and inner blue ellipse the combined Euclid probes. The inner red ellipse is the combined Euclid and Planck constraints. The square denotes Λ CDM and diamond DGP in parameter space, with the dotted line connecting them showing where extended DGP models lie. b. (right) Similar constraints in the growth index, γ_m , and w_p .

(cf. L. Amendola, M. Kuntz)

The most general (linear, scalar) metric at first-order

$$ds^2 = a^2[(1 + 2\Psi)dt^2 - (1 + 2\Phi)(dx^2 + dy^2 + dz^2)]$$

At the linear perturbation level and sub-horizon scales

Full metric reconstruction at first order requires 3 functions

$$H(z) \quad \Phi(k, z) \quad \Psi(k, z)$$

▪ modified Poisson's equation $k^2\Psi = -4\pi Ga^2 Q(k, a)\rho_m \delta_m$

▪ non-zero anisotropic stress $\eta(k, a) = \frac{\Phi + \Psi}{\Psi}$

Modified Gravity at linear level

▪ standard gravity	$Q(k, a) = 1$ $\eta(k, a) = 0$	
▪ scalar-tensor models	$Q(a) = \frac{G^*}{FG_{cav,0}} \frac{2(F + F'^2)}{2F + 3F'^2}$ $\eta(a) = \frac{F'^2}{F + F'^2}$	Boisseau et al. 2000 Acquaviva et al. 2004 Schimd et al. 2004 L.A., Kunz & Sapone 2007
▪ f(R)	$Q(a) = \frac{G^*}{FG_{cav,0}} \frac{1 + 4m \frac{k^2}{a^2 R}}{1 + 3m \frac{k^2}{a^2 R}}$, $\eta(a) = \frac{m \frac{k^2}{a^2 R}}{1 + 2m \frac{k^2}{a^2 R}}$	Bean et al. 2006 Hu et al. 2006 Tsujikawa 2007
▪ DGP	$Q(a) = 1 - \frac{1}{3\beta}$; $\beta = 1 + 2Hr_c w_{DE}$ $\eta(a) = \frac{2}{3\beta - 1}$	Lue et al. 2004; Koyama et al. 2006
▪ coupled Gauss-Bonnet	$Q(a) = \dots$ $\eta(a) = \dots$	see L. A., C. Charmousis, S. Davis 2006

New gravity,

same matter

$$X_{\mu\nu} = -8\pi G T_{\mu\nu}$$

$$T_{\mu;\nu}^{\nu} = 0.$$

$$Y_{\mu\nu} = X_{\mu\nu} - G_{\mu\nu}$$

$$G_{\mu\nu} = -8\pi G T_{\mu\nu} - Y_{\mu\nu}$$

Same gravity,

new matter

Need to break degeneracy

massive particles respond to Ψ

$$\delta'' + \left(1 + \frac{H'}{H}\right)\delta = \frac{k^2}{a^2}\Psi$$

massless particles respond to $\Phi - \Psi$

$$\alpha = \int \nabla_{\text{perp}} (\Psi - \Phi) dz$$

Correlation of galaxy ellipticities:
galaxy weak lensing

$$P_{\text{ellipt}}(k, z) \propto (\Phi - \Psi)^2$$

DGP

(Dvali, Gabadadze, Porrati 2000)

$$S = \int d^5x \sqrt{-g^{(5)}} R^{(5)} + L \int d^4x \sqrt{-g} R$$

$$H^2 - \frac{H}{L} = \frac{8\pi G}{3} \rho$$

brane

5D Minkowski
bulk:

infinite volume
extra dimension

gravity
leakage

L = crossover scale:

$$r \ll L \Rightarrow V \propto \frac{1}{r}$$

$$r \gg L \Rightarrow V \propto \frac{1}{r^2}$$

- 5D gravity dominates at low energy/late times/large scales
- 4D gravity recovered at high energy/early times/small scales

γ : perturbation growth index under gravity

$$\frac{d \log \delta}{d \log a} = \Omega_m(a)^\gamma$$

$$\gamma_s = \frac{3(1-w)}{6w-5} \approx 0.55 \quad \text{Standard}$$

$$\gamma \approx \gamma_s \left(1 + \frac{1-Q}{(1-w)(1-\Omega_m)}\right) \approx 0.65 - 0.70 \quad \text{DGP}$$

$$\gamma \approx \gamma_s \left(1 + \frac{k^2 a^2}{M(f)^2 + k^2 a^2}\right) \approx 0.40 - 0.55 \quad \text{f(R)}$$

Want, NEED! several probes for synergies and Xchecks

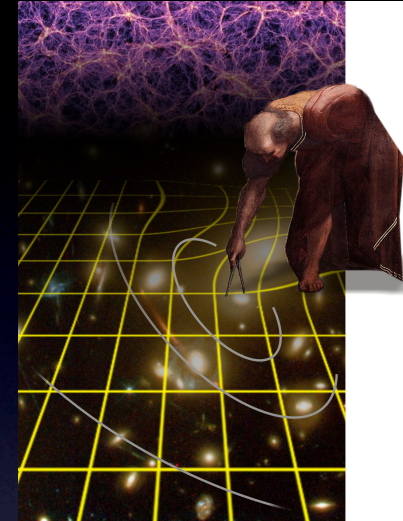
Observational Input	Probe	Description
Weak Lensing Survey	Weak Lensing (WL)	Measure the expansion history and the growth factor of structure
Galaxy Redshift Survey: Analysis of $P(k)$	Baryonic Acoustic Oscillations (BAO)	Measure the expansion history through $D_A(z)$ and $H(z)$ using the “wiggles-only”.
	Redshift-Space distortions	Determine the growth <i>rate</i> of cosmic structures from the redshift distortions due to peculiar motions
	Galaxy Clustering	Measures the expansion history and the growth factor using all available information in the amplitude and shape of $P(k)$
Weak Lensing plus Galaxy redshift survey combined with cluster mass surveys	Number density of clusters	Measures a combination of growth factor (from number of clusters) and expansion history (from volume evolution).
Weak lensing survey plus galaxy redshift survey combined with CMB surveys	Integrated Sachs Wolfe effect	Measures the expansion history and the growth

Want to measure expansion factor $H(z)$ - *geometry* - and growth of density perturbations - *dynamics* -

EUCLID

an all-sky (X_{gal}) optical/NIR mission

ESA+Euclid Consortium; EC: $\approx 900+$; Lead Y. Mellier



1. Why

1. Dark Energy & Dark Matter
(Cosmology)

2. How

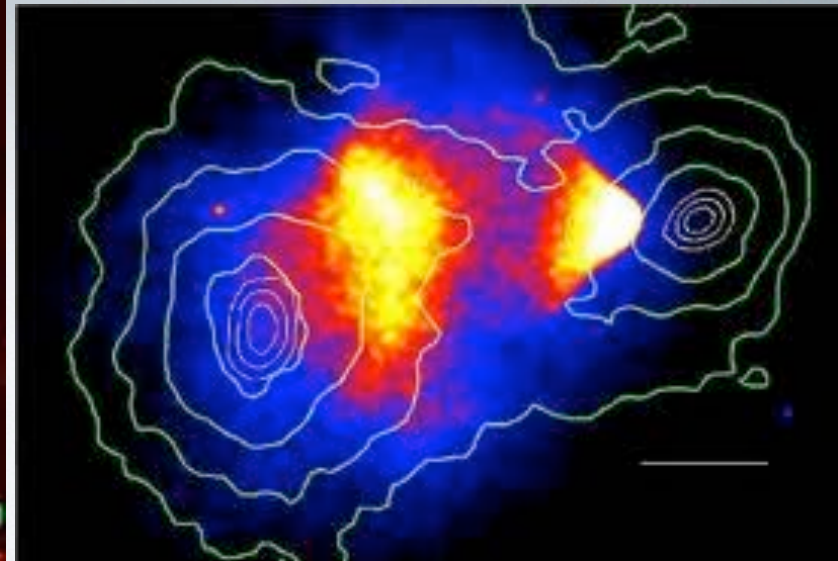
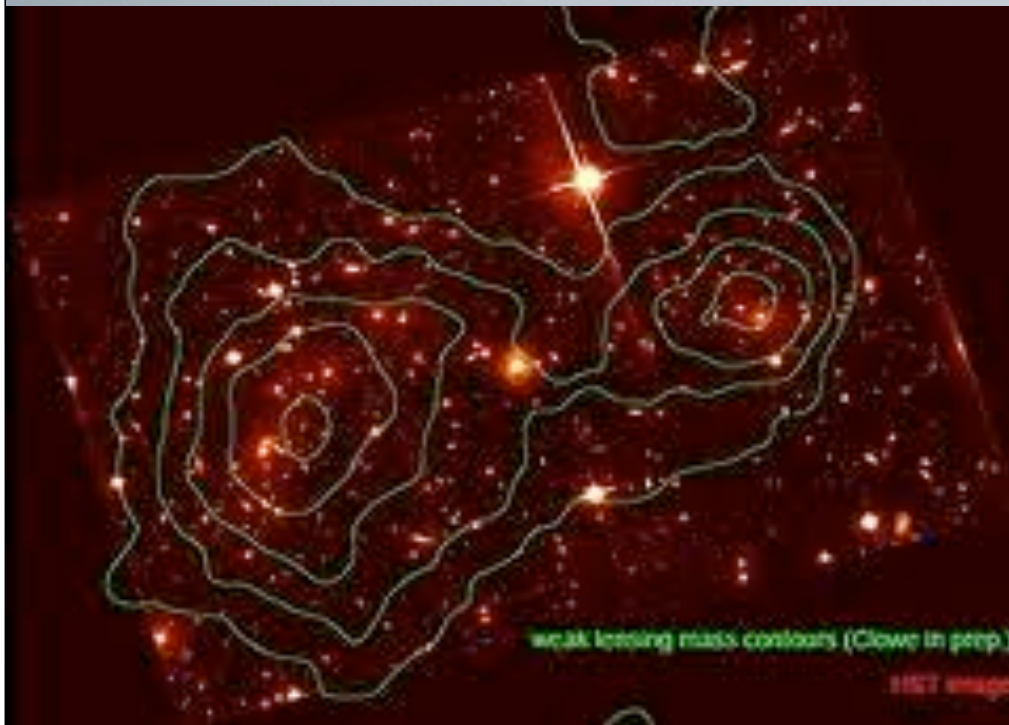
2. Space imaging (morphology & NIR)
+ Spectra: Grav. Lensing & BAO

3. When

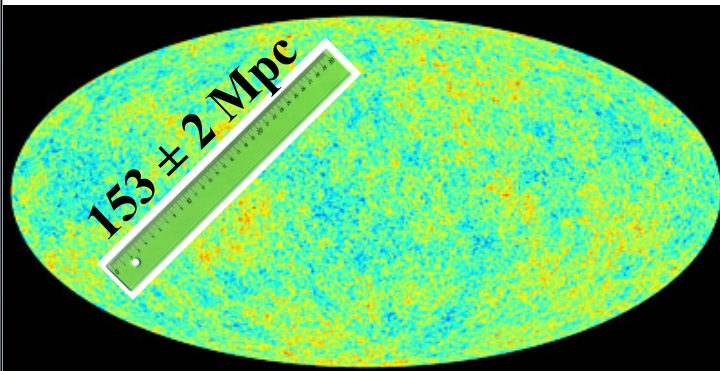
3. 2020-2025+ \sim SKA



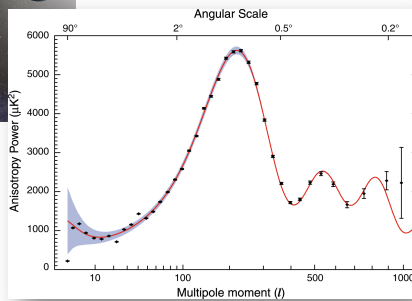
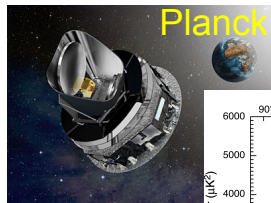
Bullet Cluster: Dark Matter!



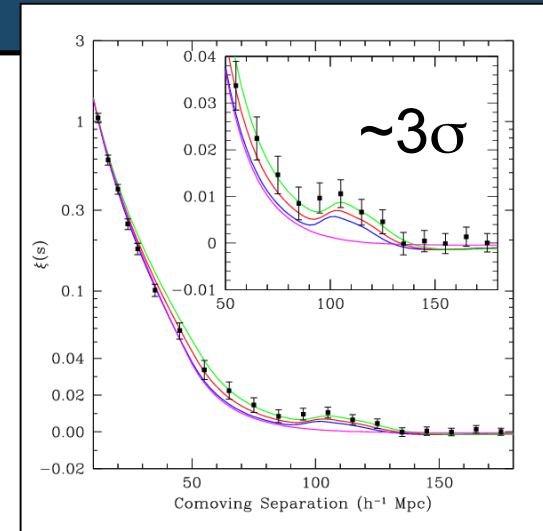
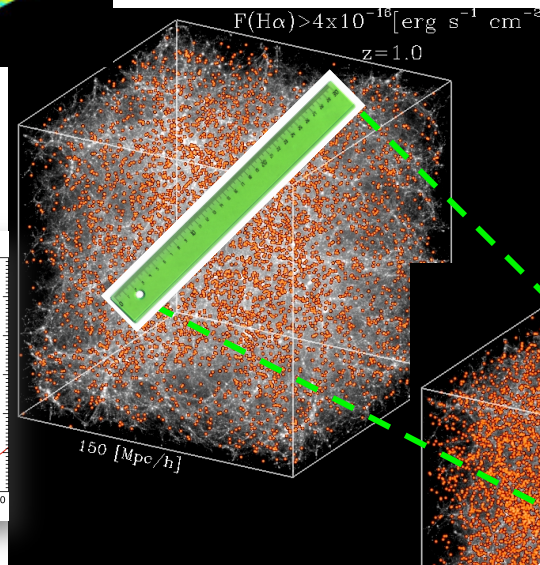
BAO as standard ruler



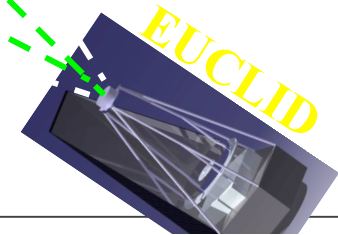
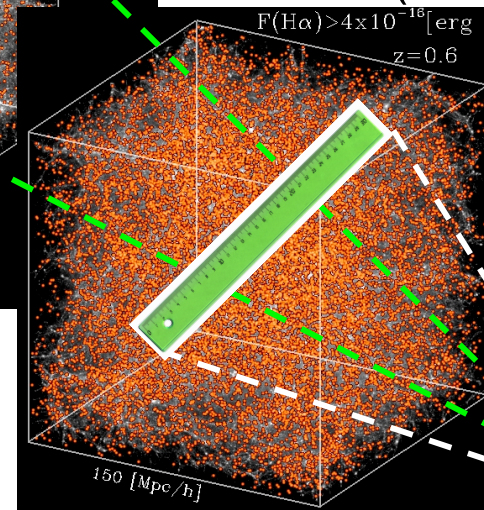
CMB ($z \approx 1000$)



Galaxies ($z > 1$)



Galaxies ($z \approx 0.35$)



- $H(z)$ (radial)
- $D_A(z)$ (tangential)
- $H(z)$ & $D_A(z)$ depend on $w(z)$

Expansion and Growth Histories through Galaxy Clustering

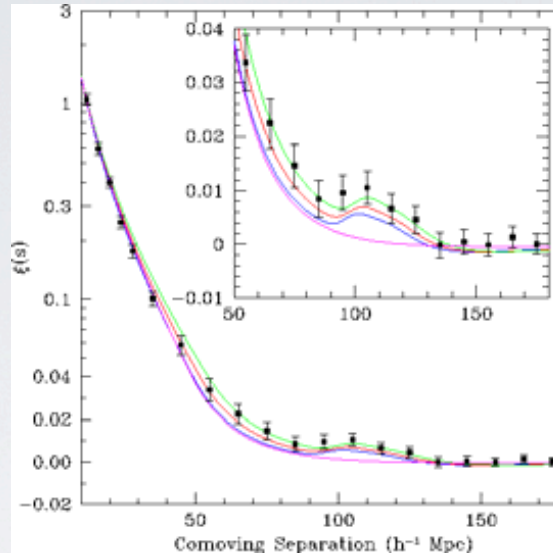
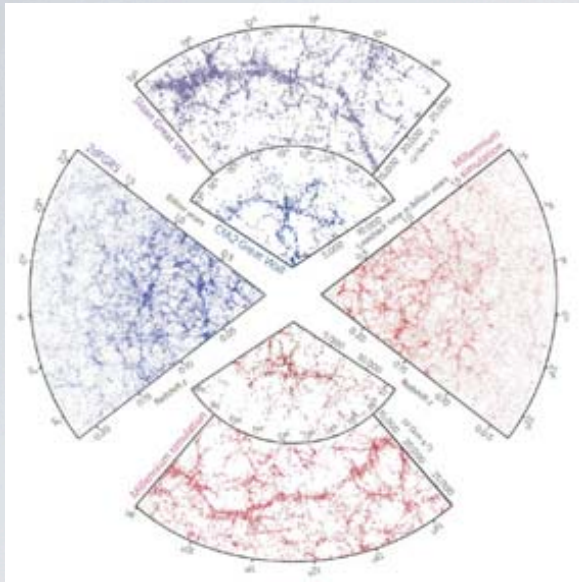
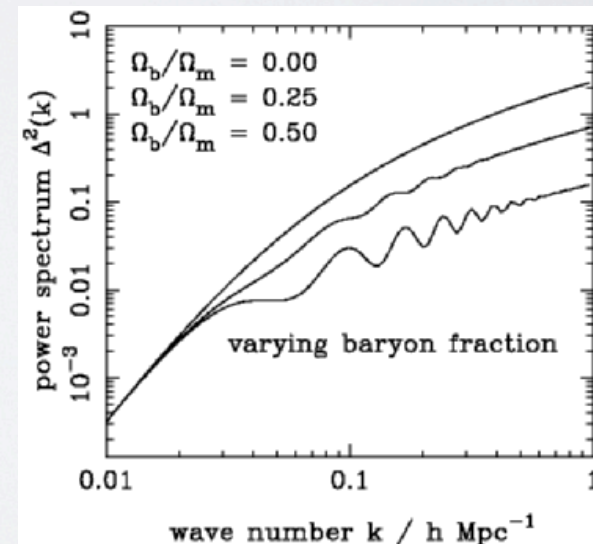


Figure 2.10: a. (Left panel) The galaxy distribution in the largest surveys of the local Universe, compared to simulated distributions from the Millennium Run (Springel et al. 2005); b. (Right panel) The two-point correlation function of SDSS “luminous red galaxies”, in which the BAO peak at $\sim 105 h^{-1}$ Mpc has been clearly detected (Eisenstein et al. 2005).

Clustering reveals features in the power spectrum of density perturbations



So far, so good..

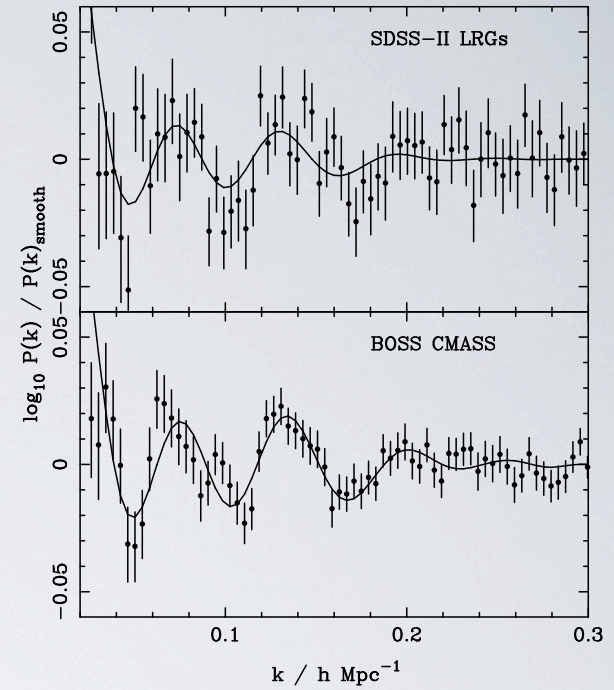
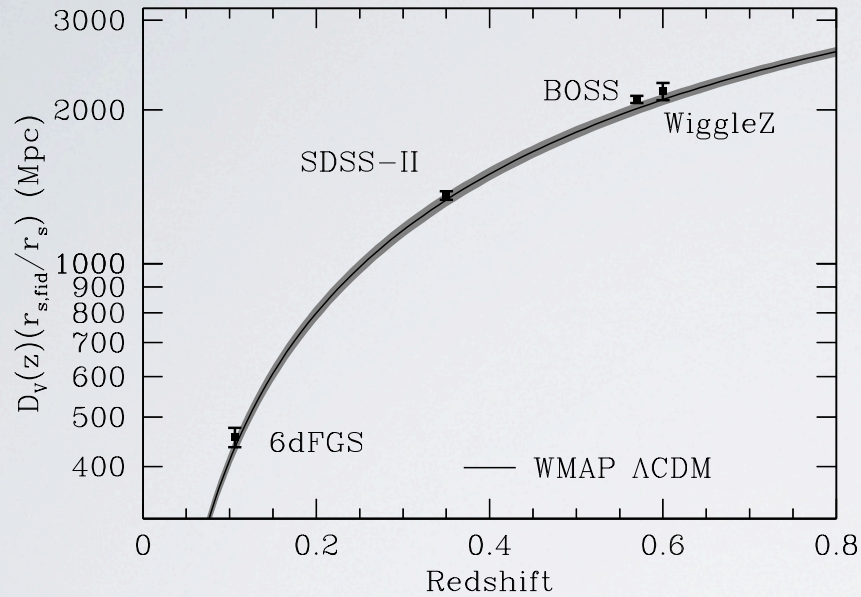
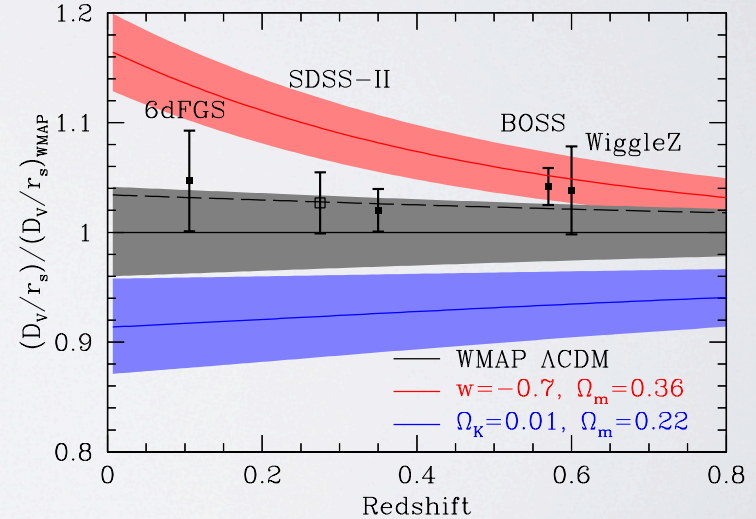
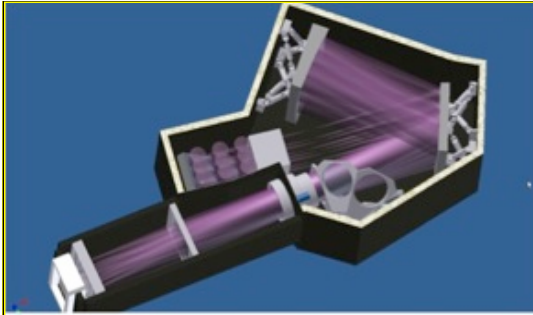


Figure 19. A plot of the distance-redshift relation from various BAO measurements from spectroscopic data sets. We plot $D_V(z)/r_s$ times the fiducial r_s to restore a distance. Included here are this CMASS measurement, the 6dF Galaxy Survey measurement at $z = 0.1$ (Beutler et al. 2011), the SDSS-II LRG measurement at $z = 0.35$ (Padmanabhan et al. 2012a; Xu et al. 2012; Mehta et al. 2012), and the WiggleZ measurement at $z = 0.6$ (Blake et al. 2011a). The latter is a combination of 3 partially covariant data sets. The grey region is the 1σ prediction from WMAP under the assumption of a flat Universe with a cosmological constant (Komatsu et al. 2011). The agreement between the various BAO measurements and this prediction is excellent.



What happens at higher z ?



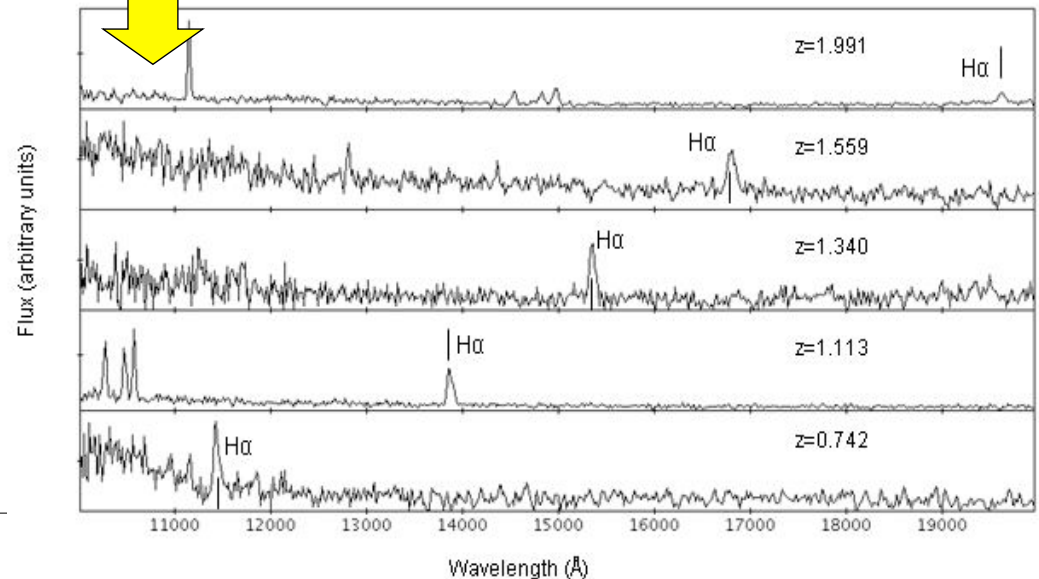
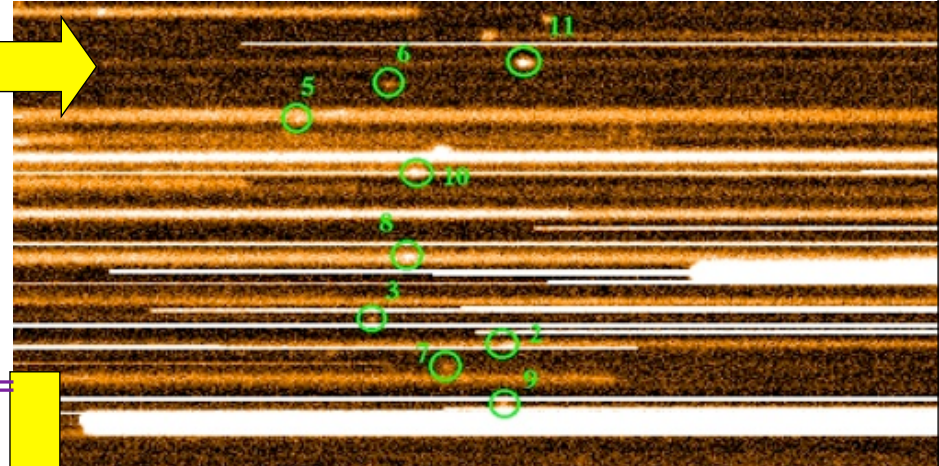
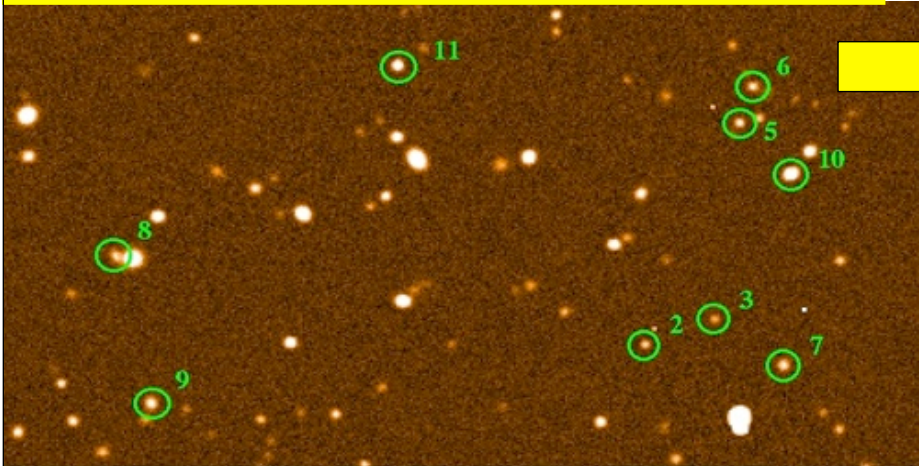
$\lambda/\Delta\lambda=300$
 1-2 μm
 FoV=0.5 deg²

Slitless spectroscopy

Simulated spectroscopic data

Main Problems:

- high backgr & confusion (rotate spectra)
- mostly emission lines (bias wrt matter? antib clusters)



- Star-forming galaxies
- $0.5 < z < 2$ ($\text{H}\alpha$)
- $F_{\text{line}} > 4 \times 10^{-16}$ erg/s/cm² ($H < 19.5$)
- $\sigma_z \leq 0.001(1+z)$
- Redshift success rate $\geq 50\%$
- $N(\text{gal}) \approx 5 \times 10^7$
- Sky coverage = 15,000 deg²
- Mission duration ≤ 6 years

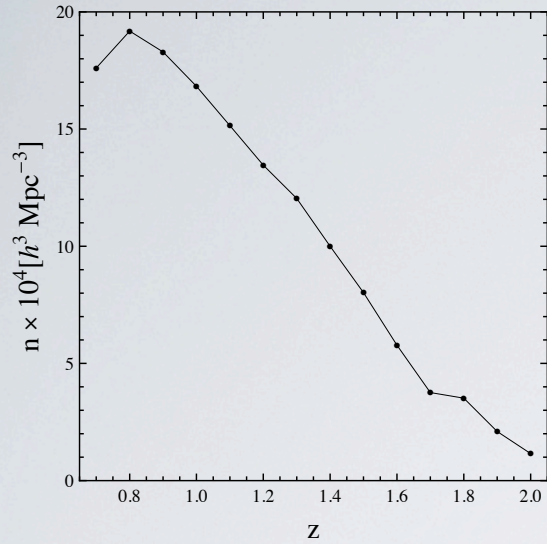


Figure 1. Predicted mean number density of galaxies in each redshift bin centred in z , expected from the baseline Euclid wide spectroscopic survey, given the instrumental and survey configurations and the estimated efficiency.

fluctuation growth

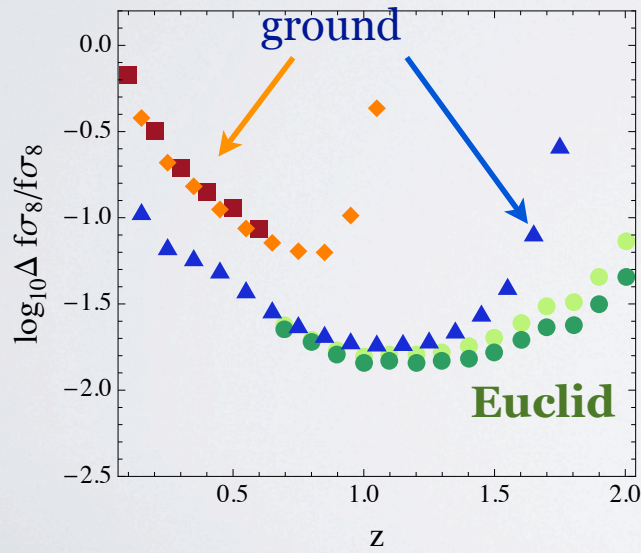
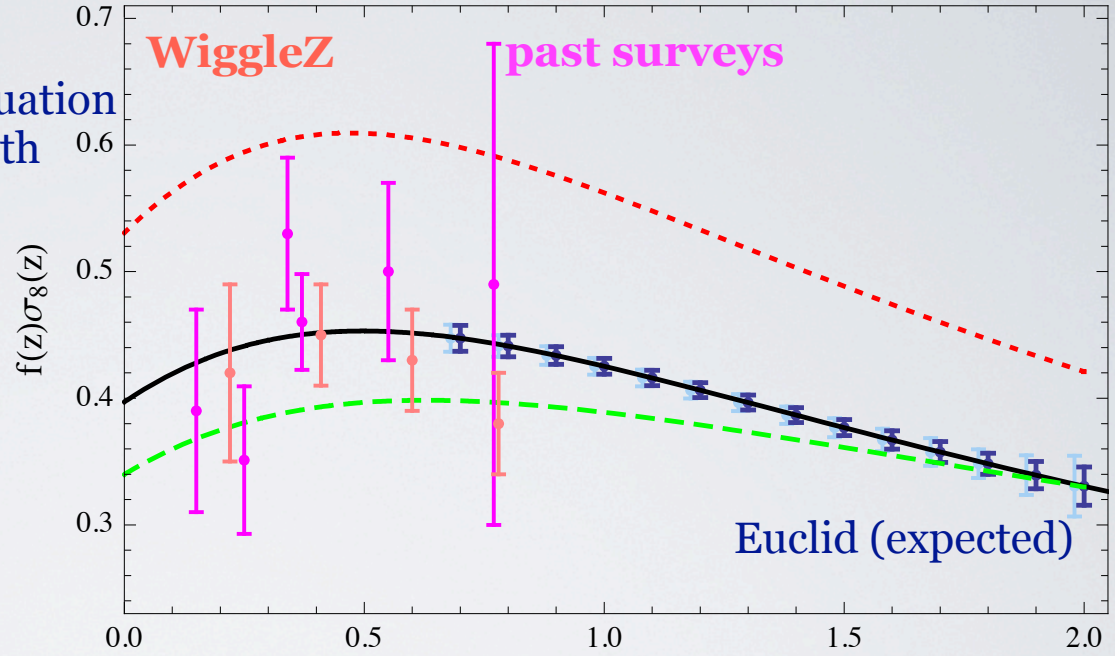
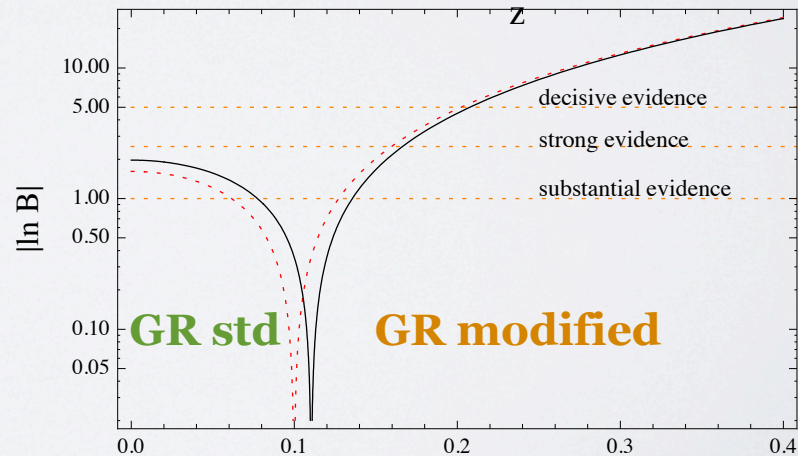


Figure 3. Relative error on $f \sigma_8$ of Euclid (dark-green circles, light-green circles for the pessimistic case of half the galaxy number density), BOSS (dark-red squares), BigBOSS ELGs (blue triangles) and LRGs (orange diamonds).



HI surveys as z-factories

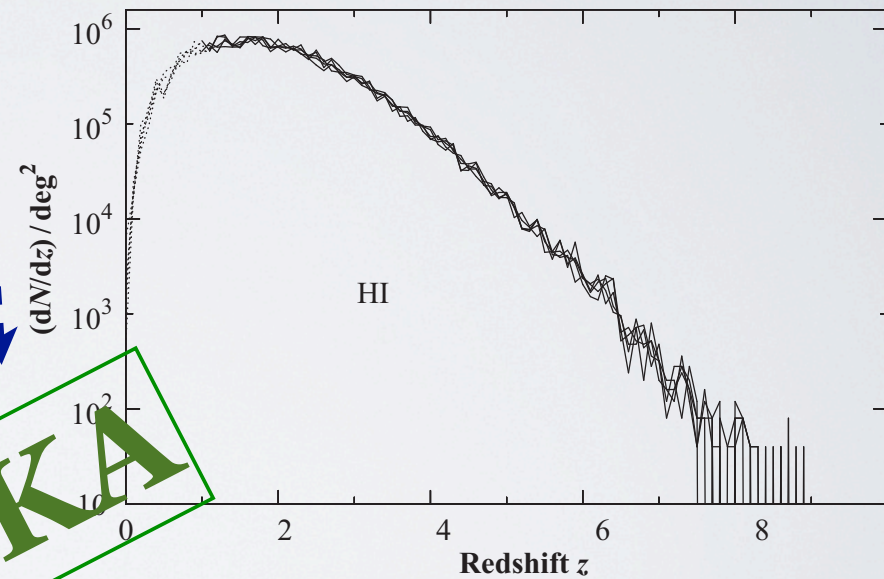
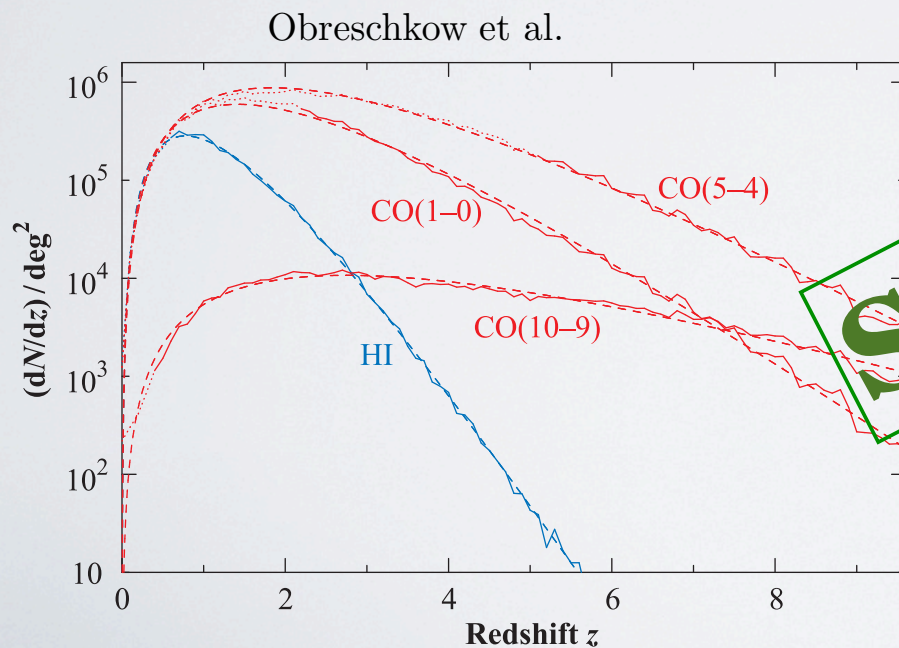
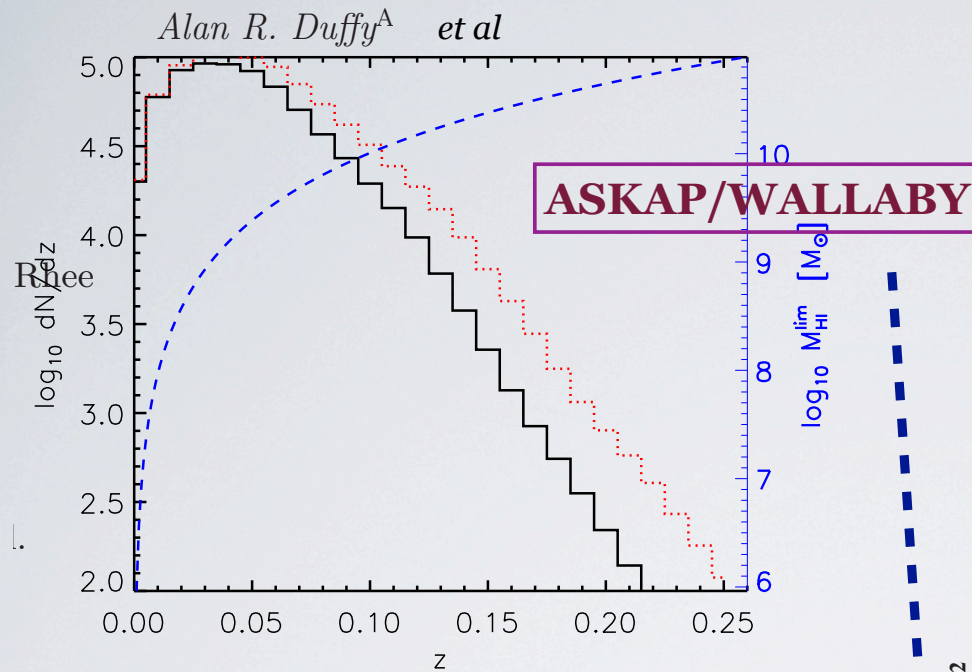
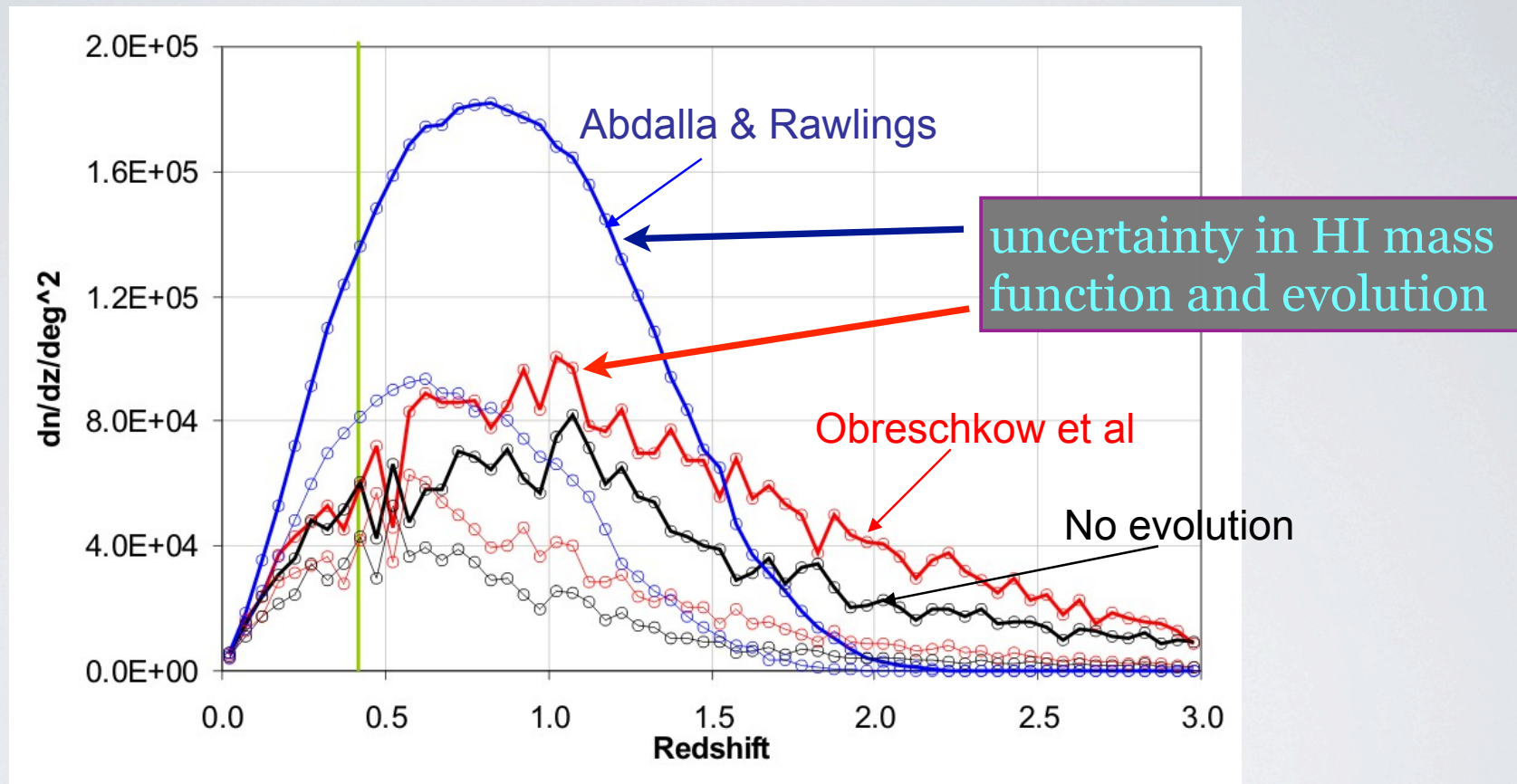


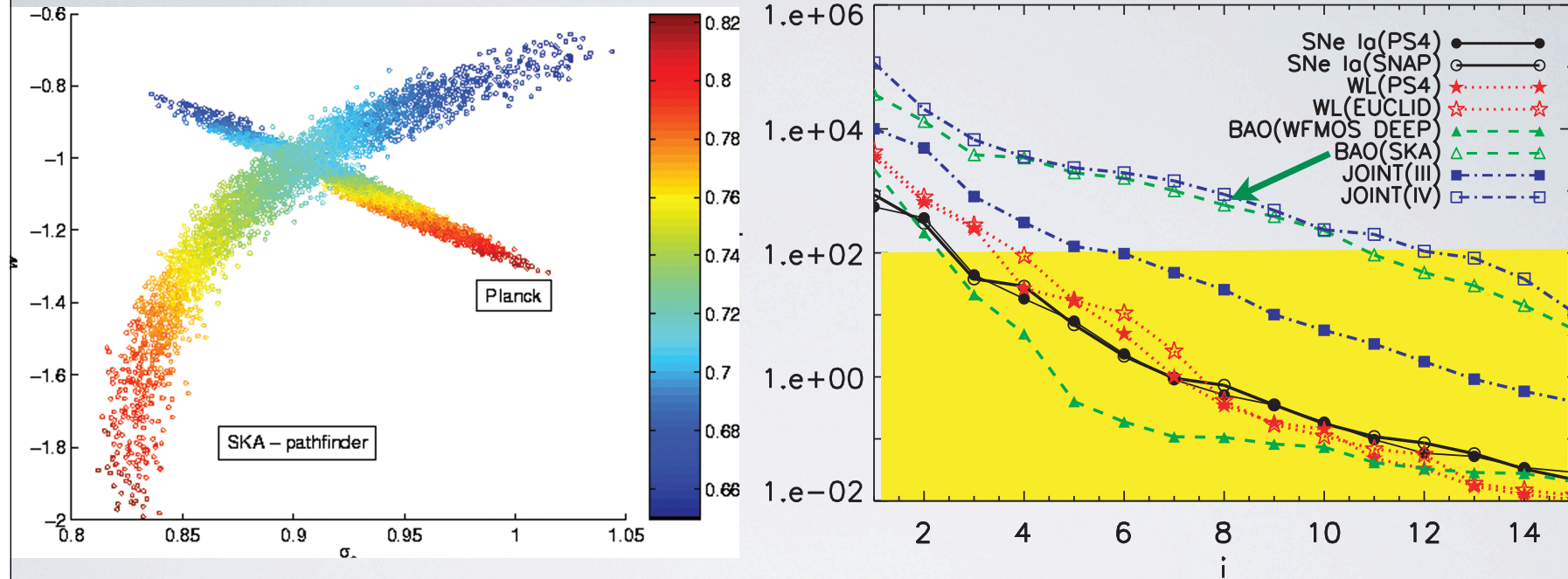
FIG. 6.— Effects of cosmic variance on a peak flux limited HI-survey with a flux limit of $1 \mu\text{Jy}$. The five lines show the dN/dz -functions extracted from five distinct random realizations of the mock observing cone (see Section 2.2). Each function uses a bin size of $\Delta z = 0.1$ and a small sky field of $1 \times 1 \text{ deg}^2$ in order to illustrate the effects of cosmic variance.

Rawlings:

SKA, not ALMA, can do many deg²



- In ~ 100 days, phased arrays deliver $>10^9$ galaxies over $\sim 20,000$ deg² to $z \sim 2$ (and multiple $P(k)$ to at least $z \sim 1$)



enormous
SKA
potential

Figure 20. The weighted eigenvalues for the surveys that we used in the joint analysis. Every line represents a survey. All the surveys are marginalized over other parameters including *Planck* priors. The (black) solid line shows SNe Ia surveys with the filled and unfilled circles indicating PS4 and SNAP, respectively. The (red) dotted lines represent WL surveys with the filled and unfilled stars indicating PS4 and EUCLID respectively. The (green) dashed lines represent BAO surveys with the filled and unfilled triangles indicating WFMOS deep and SKA, respectively. We also show the joint analysis with the (blue) dotted-dash lines; the filled and unfilled squares indicating stage III and IV, respectively.

Expansion and Growth Histories through Gravitational Lensing

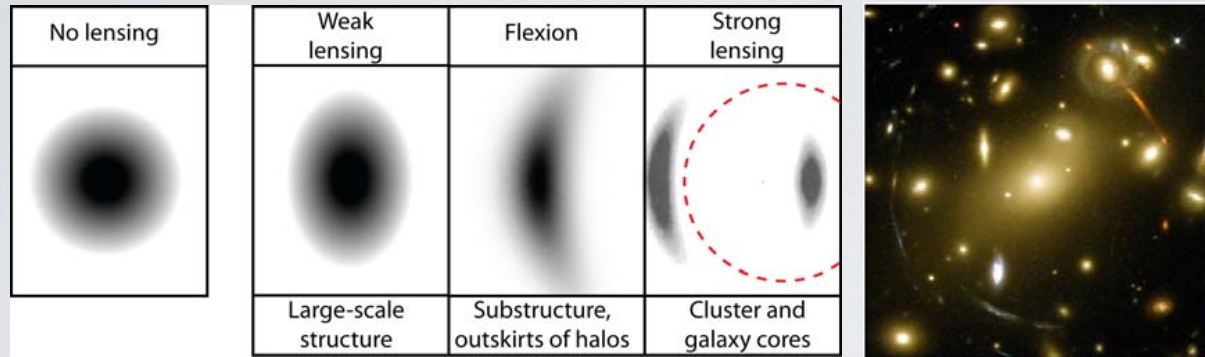


Figure 2.8: a. (Left) Illustrations of the effect of a lensing mass on a circularly symmetric image. Weak lensing elliptically distorts the image, flexion provides an arc-ness and strong lensing creates large arcs

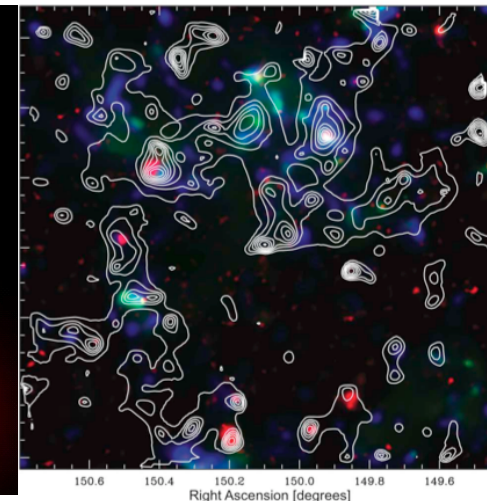
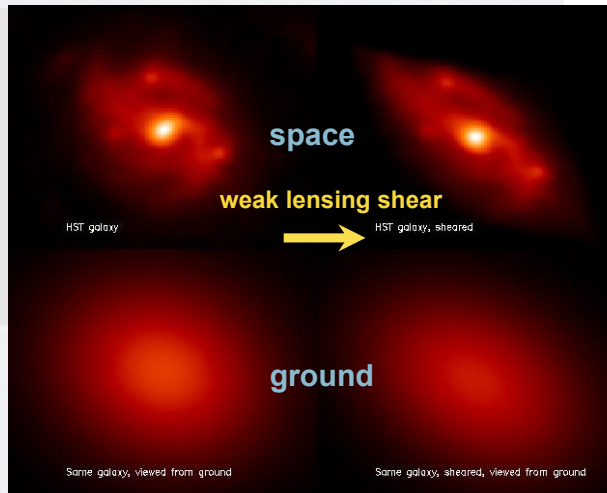
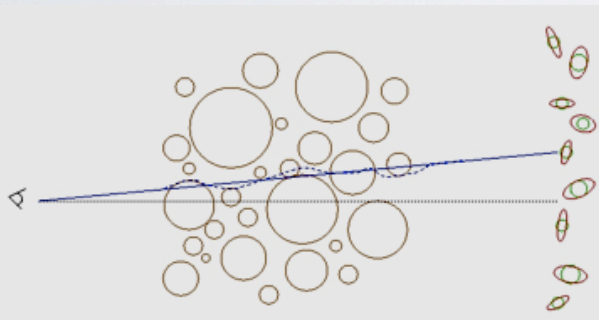
$$\kappa = \frac{3H_0^2 \Omega_m}{2c^2} \int_0^{\chi_s} d\chi \frac{D(\chi)D(\chi_s - \chi)}{\chi_s} (1+z)\delta(\chi),$$

observable

distances:
geometry

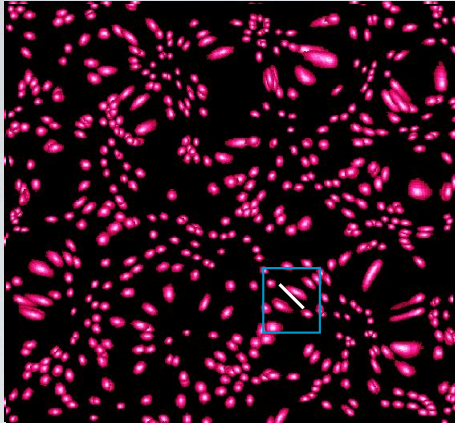
density
perturbation:
dynamics

COSMOS Dark Matter Map over 2 deg²

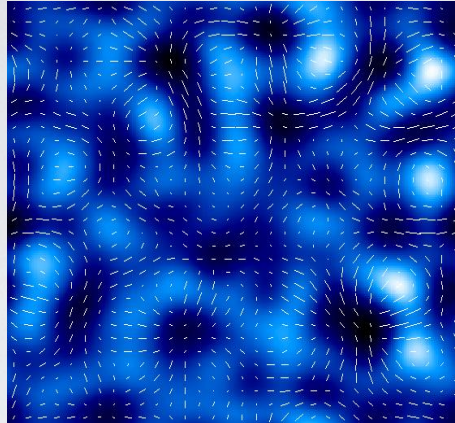


Massey et al. 2007a, Nature

Distortion matrix:
$$\Psi_{ij} = \frac{\partial \delta \theta_i}{\partial \theta_j} = \int dz g(z) \frac{\partial^2 \Phi}{\partial \theta_i \partial \theta_j}$$



lensed background galaxies



mass and shear distribution

⇒ correlated image distortions on sky produce WL power spectrum $C_l(\theta, z)$ **Weak Lensing Tomography (slices in z)** Euclid

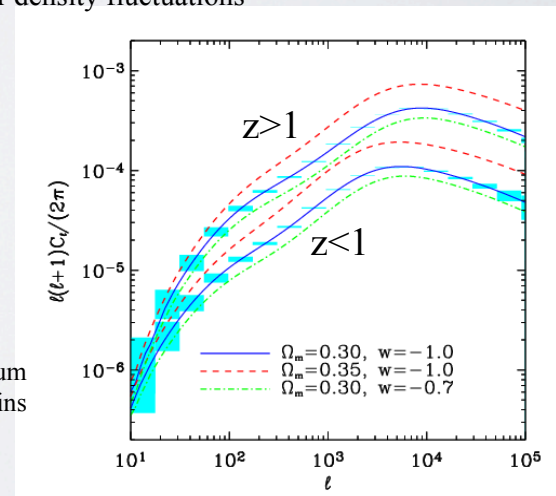
Lensing signal $C_l(\theta, z)$ depends on:

- shape of total matter density fluctuation spectrum
- angular diameter distance in lensing equation for lensing amplitude
- angular diameter distance for angular scale of density spectrum
- growth factor $g(z)$ of dark matter density fluctuations

WL tomography addresses all sectors of Dark Cosmology

need accurate $\langle z \rangle$ in bins from photoz

Example: WL power spectrum for each of two z -bins



Ground based lensing is limited by systematics

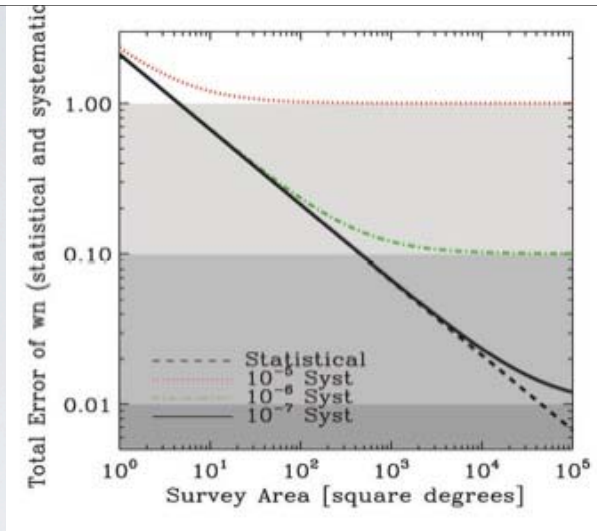
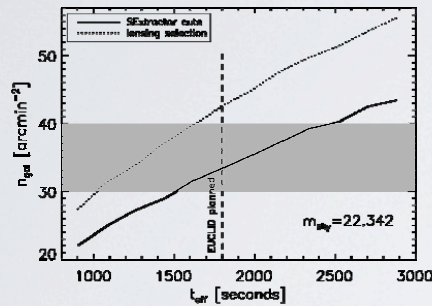


Figure 2.17: Advantages of space based observations in order to reach Euclid's cosmological objectives. The total error on the equation of state decreases statistically as the area of a survey is increased. However systematic effects limit the achievable dark energy constraint. For Euclid to achieve 2% on the dark energy equation of state requires an area of 20,000 square degrees and shape systematic levels with a variance of 10^{-7} (Cf. Amara & Réfrégier 2008). Such a systematic precision can only be achieved with the stability and accuracy of space-based observations.

For photo-z need optical colors from ground based surveys (more systematics)

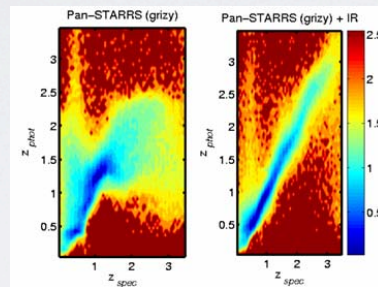


Figure 2.18: a. (Left) The expected number counts of galaxies useful for lensing as a function of exposure time. The solid line is made using a simple cut on SEExtractor detection with $S/N > 10$ and $FHWM[gal] > 1.25FHWM[PSF]$, the dashed line is from the shape measurement pipelines that sum the lensing weight assigned to each galaxy, with a cut in ellipticity error of 0.1. We see that we are able to reach our requirements of 30-40 gal/amin². b. (Right) Shows the redshift measurement for PanSTARRS with and without the Euclid NIR bands (c.f. Abdalla et al 2007). We find that with DES, PanSTARRS-2 and a fortiori PanSTARRS-4 and LSST we will be able to meet our requirements of $\delta z = 0.05(1+z)$.

NIR is mandatory for accurate photoz for

$$1 < z < 3$$

Throw away uncertain ones!!!!

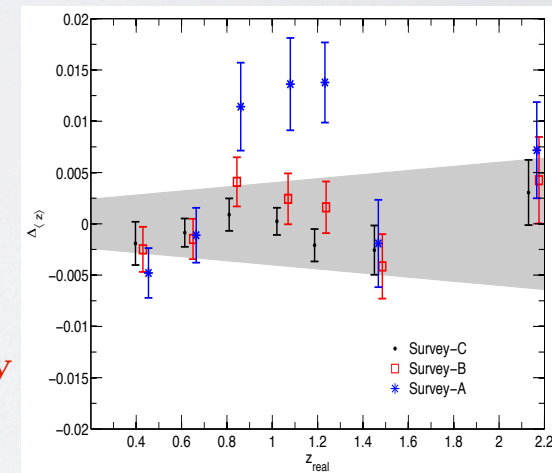


Figure 5. The bias in the mean of the tomographic bins estimates from the Normalized $\sum L(z)$ functions for survey-C and survey-A and survey-B. For survey-C, with cleaning for catastrophic failures and after applying correction gives $|\Delta_{(z)} / (1+z)| \leq 0.002$. Here the shaded region is $|\Delta_{(z)}| = 0.002(1+z)$. We have introduced a small offset in x-axis values of survey-B and survey-C for legibility. R. Scaramella - Sesto 2010

$(\frac{\sigma_z(z)}{1+z})$ for different surveys in the range $0.3 \leq z \leq 3.0$

Survey	Before Cleaning	After Cleaning	After Cleaning + Correction
Survey-A	0.1703	0.0884	0.0675
Survey-B	0.1164	0.0640	0.0497
Survey-C	0.0876	0.0492	0.0398

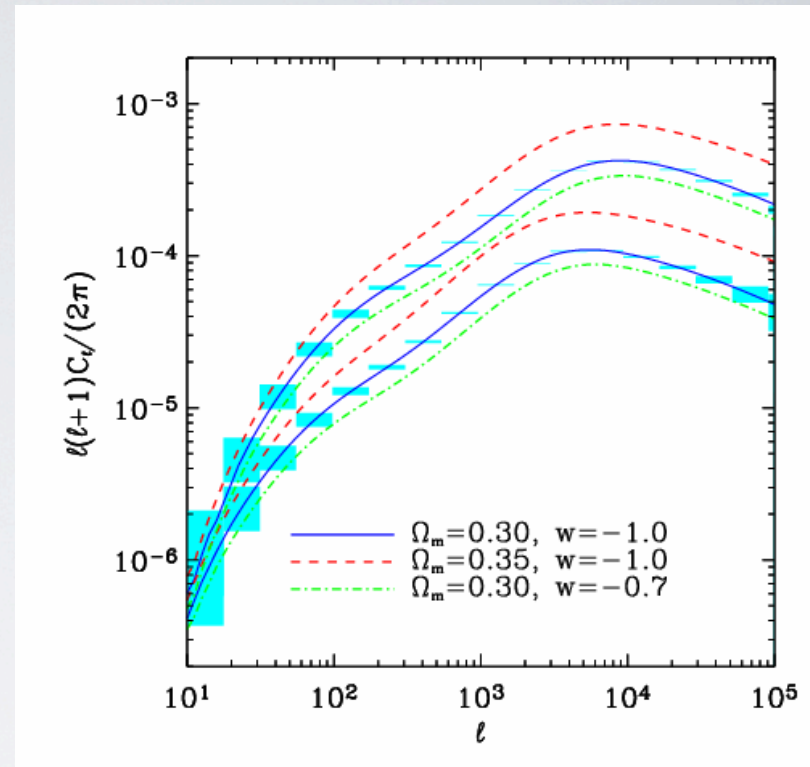
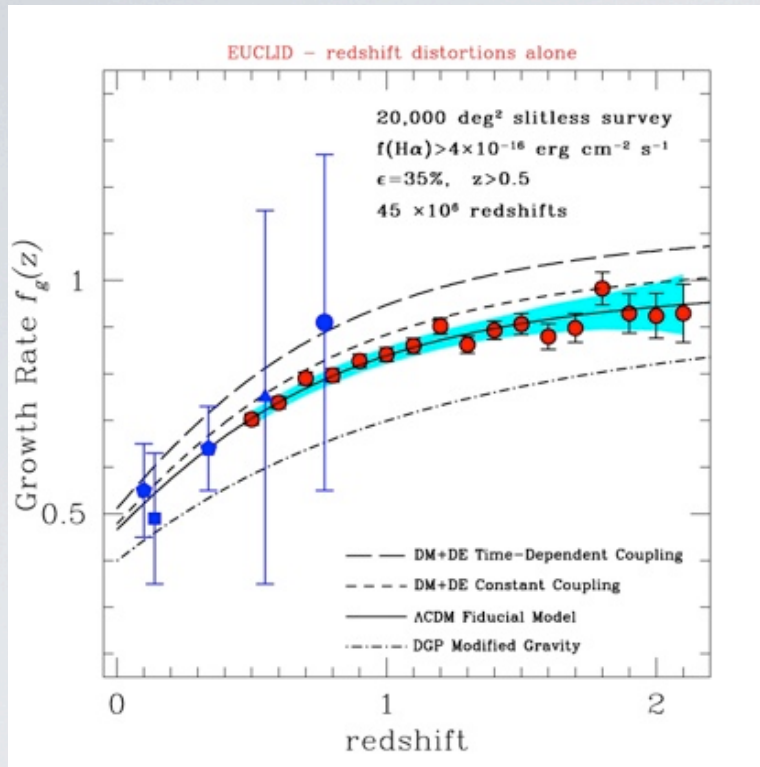


Figure 2.14: a. (left) *The growth rate of matter perturbations* as a function of redshift. Data points and errors are from a simulation of the spectroscopic redshift survey. The assumed Λ CDM model, coupled dark matter/dark energy modes and DGP are also shown. b. (right): *The predicted cosmic shear angular power spectrum at $z=0.5$ and $z=1$ for a number of cosmological models*

Powerful combination for cosmology

[Dark Energy, Dark matter, non std GR]

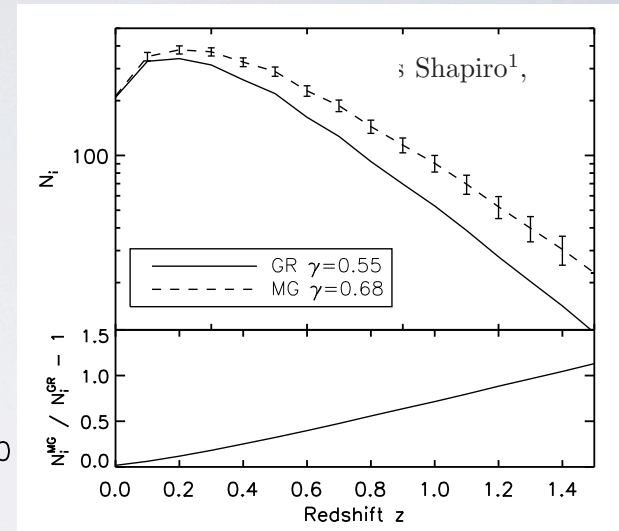
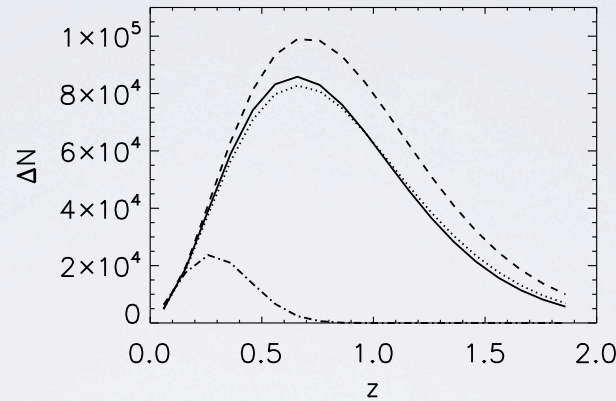
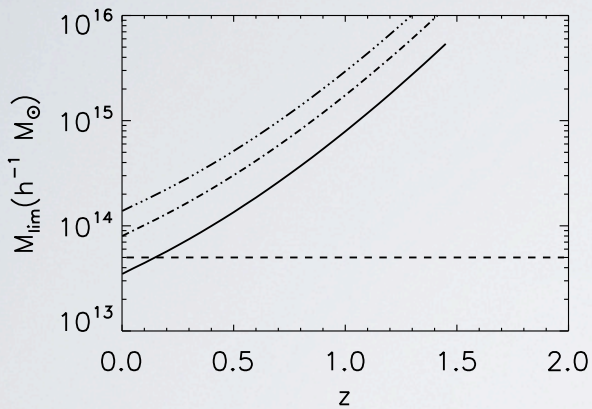
Counts & mass function (calibrate!!)

Clusters of galaxies

NIR photom (24.5), WL, (vel disp.)

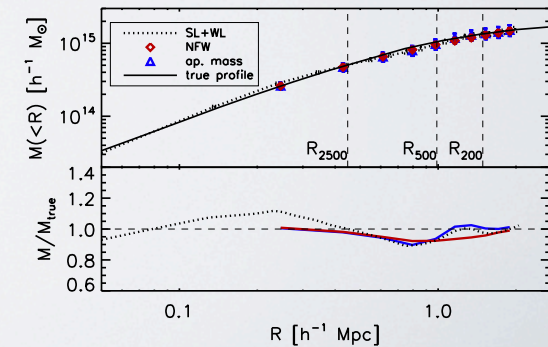
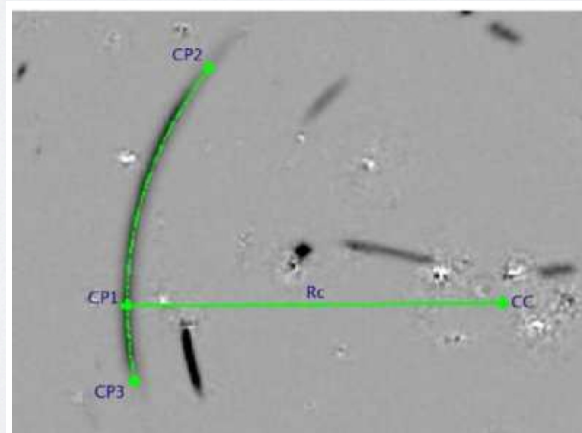
expect $N \sim \text{few} \times 10^5$

strong synergy with X, SZ



Strong lensing

Mass profile in inner regions; frequency of arcs



High
redshift
($z \sim 1$)
cluster as
seen from
Euclid
(Meneghetti et al.)



Euclid Survey Areas, (N.B. work in progress ~2 weeks ago)

$N \sim 1.5-2 \cdot 10^9$ Weak Lensing
sampling

$N \sim 5-6 \cdot 10^7$ ditto for
Clustering

J. Amiaux (ESAC tool)

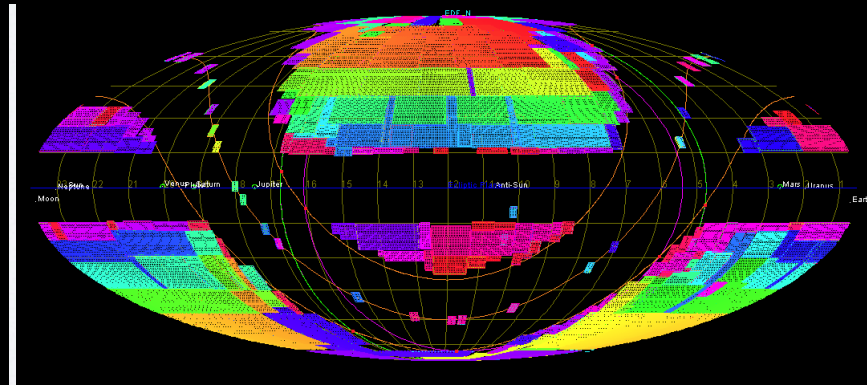
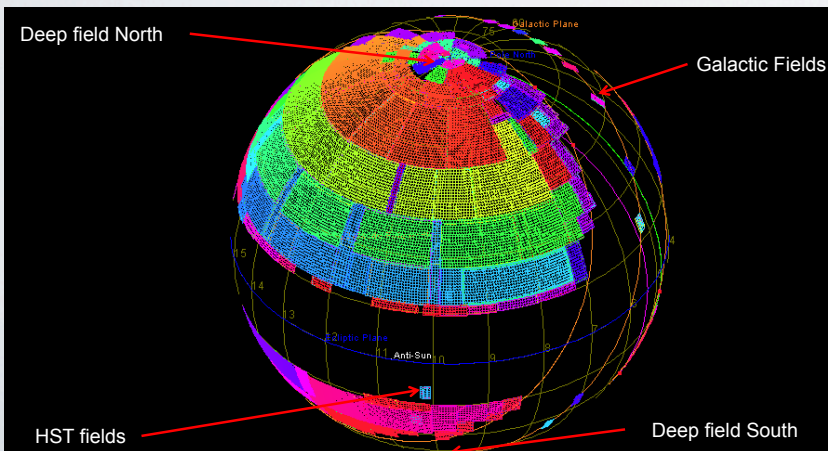
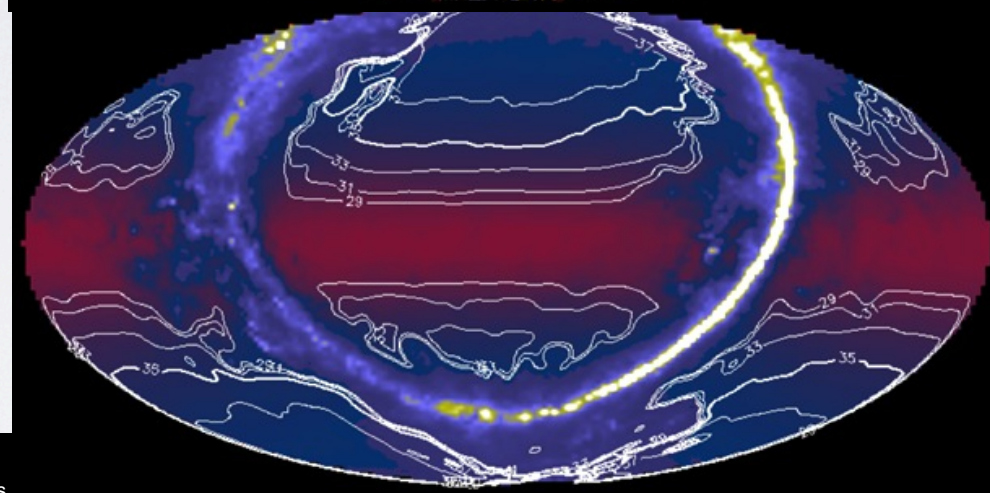
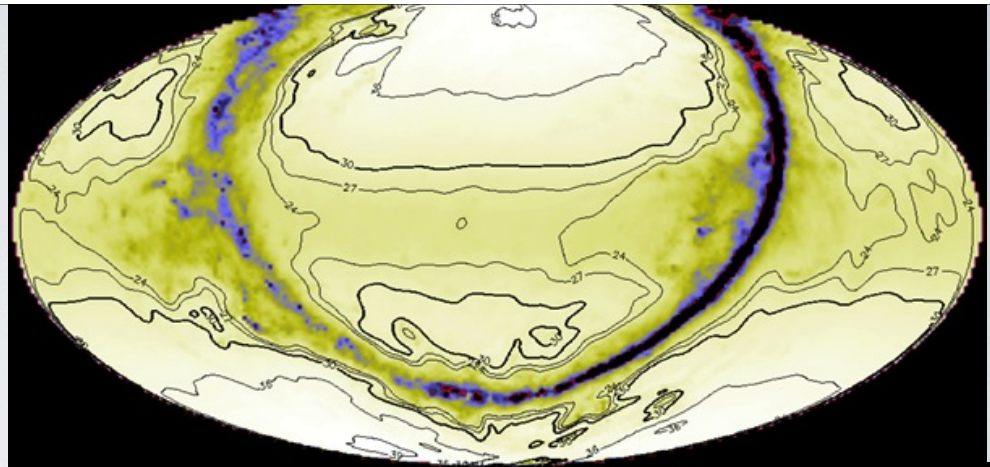


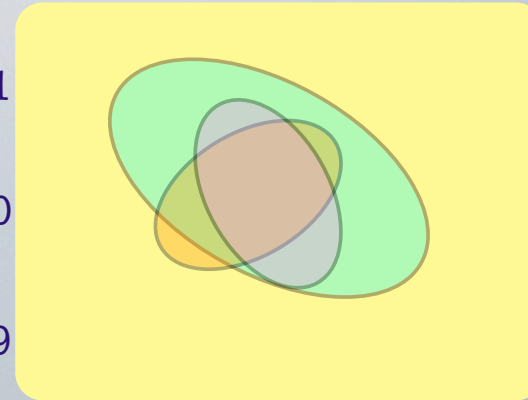
Figure 3.11.4-2: Assumption for locations of main calibrators for building the reference survey and implementation of the fields on the reference survey.

Figure 3.11.4-3: Mollweide representation of the full reference survey (including location of calibration fields).
R. Scaramella - SKAItaly June 2012

Possible outcomes.....

Quite useful but
a bit dull....

W
-1.01
-1.00
-0.99

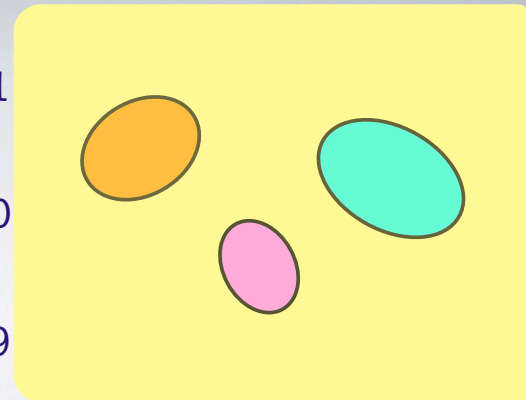


const= Λ

Ω_m

Much more
interesting!!

W
-1.01
-1.00
-0.99



?!?!?

Ω_m

Summary:

**Synergies, X-checks
& competition on**

- ★ **BAO**
- ★ **LENSING**
- ★ **LSS**
- ★ **X-IDs**
- ★ **redshifts**
- ★ **morphologies**
- ★ **NIR photom.**
- ★ **Data mining**
- ★ **etc.**

Euclid looks nice...
but what about SKA?

Highlight complementarity

Euclid:

- **Dark Matter**
- **Processed Baryons**

SKA:

- **Unprocessed Baryons [HI]**

Both have many years to go (and of work)...

But are among the **best** experiments !!

END